Available online at www.sciencedirect.com
SCIENCE DIRECT®

Journal of the European Ceramic Society 23 (2003) 2867–2877
www.elsevier.com/locate/jeurceramsoc

Sliding wear of ceramics and cermets against steel

Koji Kameo[a,*], Klaus Friedrich[a], José F. Bartolomé[b], Marcos Díaz[b], Sonia López-Esteban[b], José S. Moya[b]

[a]*Instutut für Verbundwerkstoffe GmbH (IVW), Universität Kaiserlautern, Erwin-Schrödinger-Str. Geb.58, 67663 Kaiserslautern, Germany*
[b]*Instituto de Ciencia de Materiales de Madrid (ICMM), Consejo Superior de Investigaciones Cientificas (CSIC), Cantoblanco, 28049 Madrid, Spain*

Abstract

The wear resistance of ceramics and ceramic/metal hybrid composites against steel was studied under dry sliding condition by the use of a pin-on-disc type wear test. The results were compared not only on the basis of the specific wear rates of the various ceramic based materials, but also on the basis of the total cumulative wear rates, which show accumulated wear losses of both sample material as a sliding body and its steel counterpart. From this point of view, it can be considered whether the tribo-materials are optimised with regard to the whole tribo-system or not. The specific wear rates of metal and ceramic/metal composites showed roughly 1.7–16 times higher values than the monolithic ceramics. But the total cumulative wear rate of the ceramic/metal composite, which contained larger sized metal particles, exhibited more than twice better total wear performance than the other systems. The mechanisms responsible for these behaviours were discussed by means of microscopical observations on the worn surfaces and the microstructures of the samples.

Keywords: Composites; Grain size; Mullite/molybdenum; Wear resistance; Zirconia/nickel

1. Introduction

Since engineering ceramics possess superior wear and heat resistance, advanced ceramic-based materials are increasingly being used to design wear resistant components in fuel systems, composite brake rotors and valves for automobiles and aircrafts. This is especially true for engine parts, for which a more efficient combustion and a significant fuel savings can be achieved with these materials.[1,2] New technologies often require that components have to perform multiple functions or exhibit characteristics, which are not attainable by any single phase material currently available. In this sense, dissimilar materials, like metals and ceramics, can be applied together to obtain an optimum combination of their properties such as high hardness, strength and toughness. In metal-reinforced ceramic, the utilisation of the inherent toughness of the second-phase particles is determined by the interfacial properties and nature of the internal stress.[3–5] Good interface bonding between the brittle matrix and the ductile phase leads to extensive plastic deformation of the ductile phase, and, is therefore conductive to the toughening of the composites. Thus, key factors in selecting suitable reinforcement materials are chemical compatibility with the matrix and the thermal expansion coefficient, which must be similar to the one of the matrix.

In the long years of research on the tribology of materials, numerous wear phenomena and mechanisms have been demonstrated and discussed. Detailed descriptions are found for example in Refs. 6–12. Even apart from engineering mechanisms, there are many other areas where wear loss of material is commonplace all over our daily life. Since wear phenomena change drastically even with a relatively small change in a tribosystem, caused by dynamic, material and/or environmental parameters, it's often remarked as the following saying[12]:

> Wear is not a material property. It is a system response.

The complexity of wear means that, in general, only a few reliable predictions regarding the wear of composites can be made. In this sense, a number of works have to be stored up in order to construct a diversified database on

* Corresponding author. Tel.: +49-631-2017-217; fax.: +49-631-2017-196.
E-mail address: kameo@ivw.uni-kl.de (K. Kameo).

0955-2219/03/$ - see front matter © 2003 Elsevier Ltd. All rights reserved.
doi:10.1016/S0955-2219(03)00297-8

wear of composites. The friction and wear behaviour of ceramics and ceramic/metal composites has, however, not been studied very well, especially with regard to sliding against steel counterparts, although steel is the most popular and necessary material in industry. Even a relatively small amount of wear debris can cause a catastrophic failure of large and complex devices. For example, when a small sliding body is placed on a huge massive steel component in a mechanical system and, thus, this steel component should not be replaced so often due to wear, the small sliding body must be designed and optimised, prior to the application of lubricants. In this respect, an incorporation of metal in the small ceramic body might bring about positive effects. Several interesting reports with regard to this matter can be found for example in Refs. 13–15. The aim of this study was therefore to further investigate the tribological behaviour of ceramic/metal composites against steel under dry sliding conditions, with the objective to develop smart tribo-materials and/or systems. This paper presents the preliminary results of an investigation of the wear of two different ceramic–metal systems: (a) mullite–molybdenum with a strong ceramic–metal interface[16,17] and (b) zirconia–nickel where the metal inclusion is weakly bonded to the matrix.[18]

2. Material preparation

2.1. Starting materials

The following commercially available powders have been used: (1) 99.9% pure Mo metal (Goodfellow Cambridge Ltd., UK), labelled Mo-3, with an average particle size of 3 μm and a specific surface area of 1.3 m^2/g; (2) 99.95% pure Mo metal (H. C. Starck, Germany), labelled Mo-9, with an average particle size of 9 μm and a specific surface area of 0.7 m^2/g. Oxygen contents below 1 wt.% in all Mo powders were detected. (3) Mullite (Scimarec Ltd., Japan) with an average particle size of 1.5 μm, a specific surface area of 7 m^2/g, and with chemical analysis (wt.%), Al_2O_3 (71.5), SiO_2 (27.3), Na_2O (0.02), MgO (0.04), CaO (0.07) and Fe_2O_3 (0.05); (4) tetragonal zirconia polycrystals (3 mol% yttria-doped) (Tosoh Corp., Japan) with an average particle size of 0.3 μm and a specific surface area of 6.7 m^2/g; (5) 99.9% pure Ni metal (Kawatetsu Mining Co., Ltd., Japan), labelled Ni-2, with an average particle size of 1.5 μm, a specific surface area of 1.7 m^2/g and an oxygen content of 0.5 wt.%.

2.2. Powder technology and sintering processes

In order to obtain mullite–molybdenum composites, different suspensions were prepared by mixing of mullite powder with 32 vol.% of Mo-3 and Mo-9 powders, using distilled water as a liquid medium. The solids loading was fixed to 70 wt.% (30 vol.%) and an anionic polyelectrolyte (Dolapix PC-33, Zschimmer & Schwarz, Germany) was added (1 wt.% referred to total solids loading) as a deflocculant. The mixtures were homogenised by milling with zirconia balls in polyethylene containers at 150 rpm for 24 h and then dried at 90 °C for 24 h. The resulting powders, labelled Mu/Mo-3 and Mu/Mo-9, were crushed in an agate mortar and passed through a 100-μm sieve. Then the powders were reduced using a 90% Ar/10% H_2 atmosphere at 1000 °C for 2 h and hot-pressed in a carbon die of 50 mm diameter at 1650 °C and 45 MPa thereby, avoiding the contact with oxygen. Discs with a diameter of 50 mm and a thickness of 13 mm were obtained. For a comparative purpose, a similar experimental procedure was applied to obtain monolithic mullite compacts, labelled Mullite. In both cases, the average grain sizes of mullite in the sintered compacts were determined as 2.4 μm with platelike grains by the aid of the linear intercept method.

Zirconia/nickel composites (ZrO_2/Ni-2) containing 30 vol.% of Ni, were prepared from suspensions with a solids content of 70 wt.% using distilled water as a liquid medium and 3 wt.% addition of Dolapix PC-33 as a deflocculant. The mixture was homogenized by milling with zirconia balls in polyethylene containers at 150 rpm for 24 h and then dried at 90 °C for 24 h. The resulting powders were crushed in an agate mortar and then passed through a 100-μm sieve and finally pressed isostatically at 200 MPa. The resulting cylindrical rods of ZrO_2/Ni-2 was first reduced at 500 °C for 2 h in a 90% Ar/10% H_2 atmosphere, to remove the NiO present in the Ni starting powder, and then the rods of ZrO_2/Ni-2 were sintered at 1430 °C for 2 h in a 90% Ar/10% H_2 atmosphere, with a heating and cooling rate of 10 °C/min. For comparison a similar experimental procedure was applied to obtain monolithic zirconia compacts, labelled Zirconia. The average grain size of zirconia in the sintered compacts was 0.3 μm and the average size of the nickel inclusions was 2.1 μm by the linear intercept method.

3. Experimental procedure

The bulk densities of all the sintered samples (i.e. Mullite, Mu/Mo-3, Mu/Mo-9, Zirconia and ZrO_2/Ni-2), a flat-rolled 99.9% pure Mo (Goodfellow Cambridge Ltd., UK), a pure Ni, which was sintered from the same powder used for ZrO_2/Ni-2 and a ball-bearing steel (100Cr6, LS2542, INA-Schaeffler KG),[19] which was utilised as a counterpart material for sliding wear test, as reference materials, were measured by the Archimedes buoyancy method. A micro-hardness measurement device with a standard pyramid diamond indenter with an apex of 136° was used to determine the

Table 1
Densities and micro-hardnesses of ceramics, metals and ceramic/metal composites[a]

	Mullite	Mu/Mo-3	Mu/Mo-9	Mo	Zirconia	ZrO_2/Ni-2	Ni	100Cr6
ρ [g/ml]	3.2	5.4	5.4	10.2	5.6	5.8	8.8	7.8
$\rho_{meas.}/\rho_{th.}$	0.98	0.98	0.98	–	0.98	0.93	–	–
H_U [GPa]	10.6±0.3	7.6±1.1	7.1±1.0	3.1±0.2	7.8±1.0	3.8±0.2	0.9±0.1	6.8±1.7
H_V [GPa]	19.3±2.9	10.8±2.7	9.7±2.1	3.1±0.2	11.7±3.7	4.3±0.3	1.0±0.1	11.4±1.0

[a] Note that the hardness values were obtained with a maximum load of 600 mN.

universal and Vickers hardnesses of all the samples, of which their surfaces polished down to $R_a = 0.2$ μm. For this test a maximum load of 600 mN, a loading and unloading speed of 70 mN/s and a holding time of 5 s after completing the indentation were applied. For each sample five measurements were averaged. Both hardness values can be expressed by the following equations:

$$H_U = P/26.43h^2$$

$$H_V = 1.854P/d^2$$

The universal hardness H_U is online calculated by the penetration depth of the indenter h, whereas the Vickers hardness H_V is determined via the diagonal lengths of the indent d, as measured after indentation. This results in the fact that only plastic deformation is detected for the Vickers hardness, while both elastic and plastic deformations are considered for the universal hardness.

The produced materials were machined carefully in order to obtain prismatic bars with 15 × 3 × 4 mm^3 dimensions for sliding wear tests. The contact surfaces (3 × 4 mm^2) of the bars were polished down to $R_a = 0.2$ μm. Subsequently all the samples and steel discs as counterpart were washed ultrasonically in an acetone bath for 5 min, and then dried in an oven at 90 °C for 30 min. In order to assess the sliding behaviour of these materials, a pin-on-disc type wear test in air (ambient temperature of 21 °C and relative humidity of 50–70%) was carried out. A speed of 1.0 m/s and an apparent pressure of 1.0 MPa were applied on the sample pins, when sliding against 100Cr6 steel disc (with the surface roughness of $R_a = 0.5$ μm) over a period of 20 h. The sliding surface was parallel to the hot-pressing direction

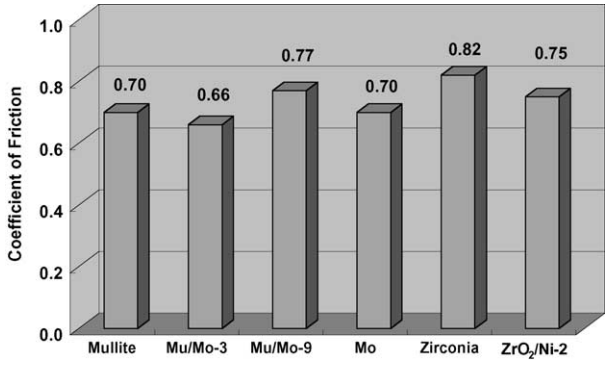

Fig. 1. Coefficients of friction of ceramics, metal and ceramic/metal composites against steel.

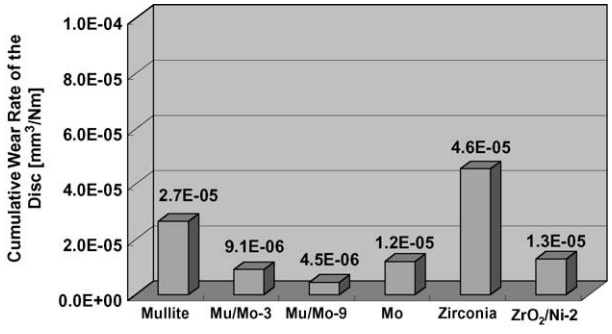

Fig. 3. Cumulative wear rates of steel discs against ceramics, metal and ceramic/metal composites.

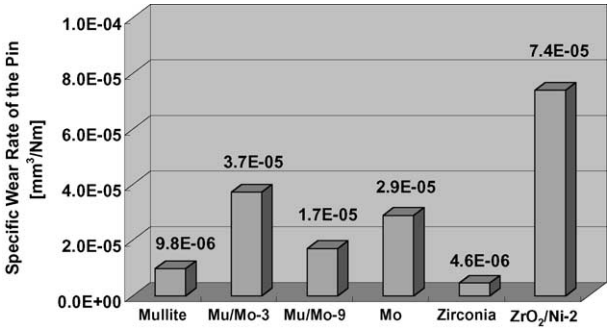

Fig. 2. Specific wear rates of ceramic, metal and ceramic/metal composite pins against steel.

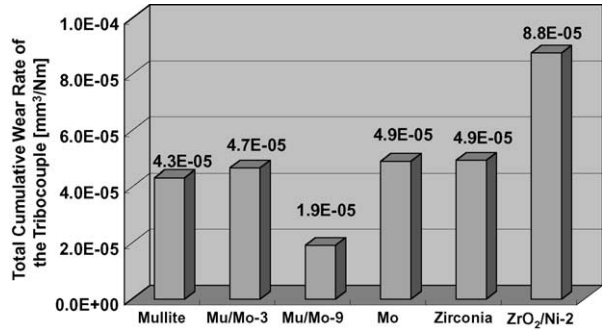

Fig. 4. Total cumulative wear rates of the tribocouples (i.e. both ceramic, metal and ceramic/metal composite pins and steel discs).

of the various materials. A frictional force induced torque was online-measured using a load cell with an accuracy of 0.1 Nm, in order to acquire the coefficient of friction μ. The specific wear rate w_S was also online-computed as the depth wear loss Δh (with an accuracy of 0.1 μm) times apparent sliding area A, divided by the applied load F_N and the sliding distance S:

$$w_S = \frac{\Delta h \cdot A}{F_N \cdot S}$$

The disadvantage of the Δh-measurement is that the depth wear loss of the disc is also taken into account as the depth wear loss of the pin. When the wear of the disc is not negligible, it should be noted that the error of the wear rate of the pin can be quite high. In such a case, it is much better to determine the cumulative wear rate w_C for each, pin and disc, by measuring the weight wear loss of each component Δm, after wear testing, divided by the corresponding density ρ, the applied load F_N and the sliding distance S:

$$w_C = \frac{\Delta m}{\rho \cdot F_N \cdot S}$$

The advantage of the cumulative wear rate is that one can measure the wear rates of both pin and disc separately. On the other hand, the cumulative wear rate cannot be measured online, and only the difference in weight before and after wear testing is taken into account. This means, the cumulative wear rate indicates only an average value of the specific wear rate, without considering changes in wear rate during testing time. The summation of the cumulative wear rates of the tribocouple (pin and disc) is referred to as the total cumulative wear rate. Three measurements were averaged for each material. For the specific wear rate, the stable value after 20 h of sliding was chosen for the discussion. So that the value has hardly any relation with the initial unstable transition of the wear behaviour, and it can be regarded as a constant of the material or the system.

The microstructures of the specimens after wear testing were studied by the use of a surface profilometer, an

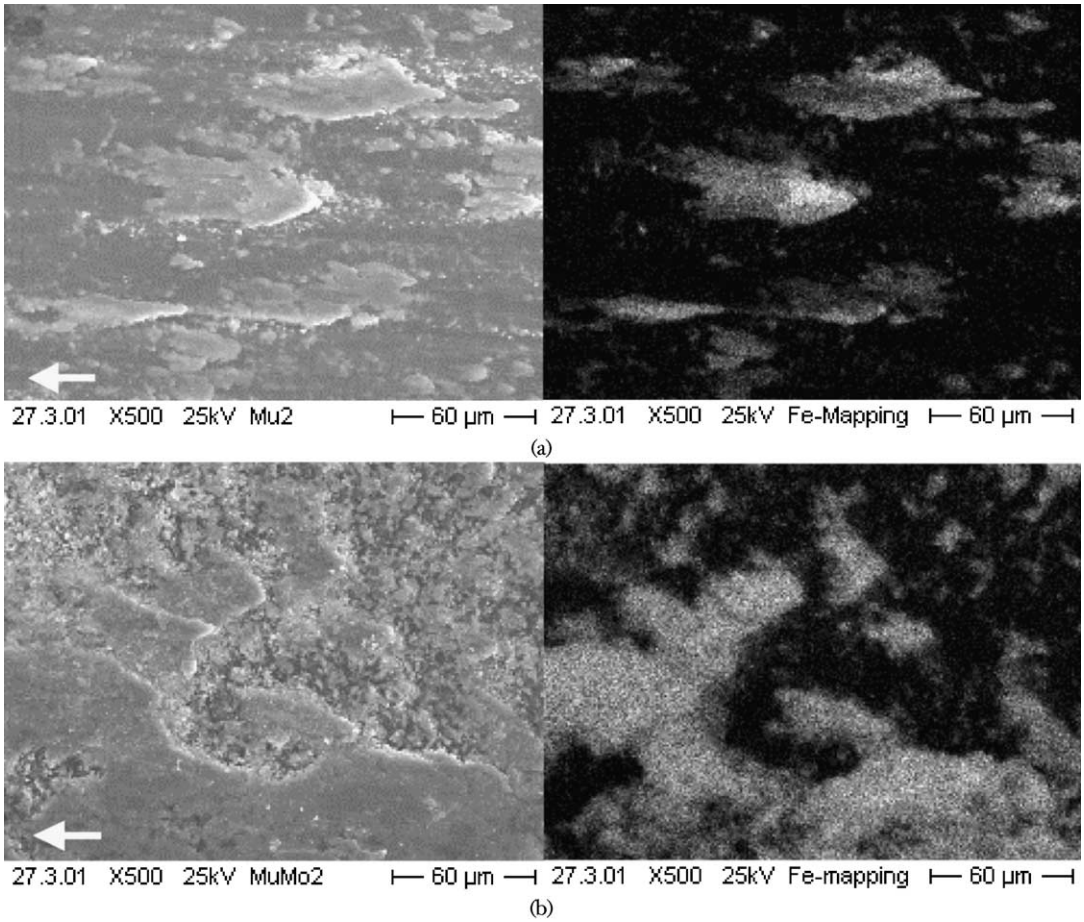

Fig. 5. The detailed worn aspects and the area distribution images of Fe-element of (a) mullite and (b) mullite/molybdenum composite (Mu/Mo-3) after 72 km sliding. The sliding direction of the pin was indicated.

optical light microscope, a scanning electron microscope with a wavelength dispersive X-ray (WDX) analysis, and an atomic force microscope (AFM). The surface roughness R_a was determined by the use of a laser surface profilometer, in accordance with the standard (DIN 4768, ISO/DIS 4287/1).

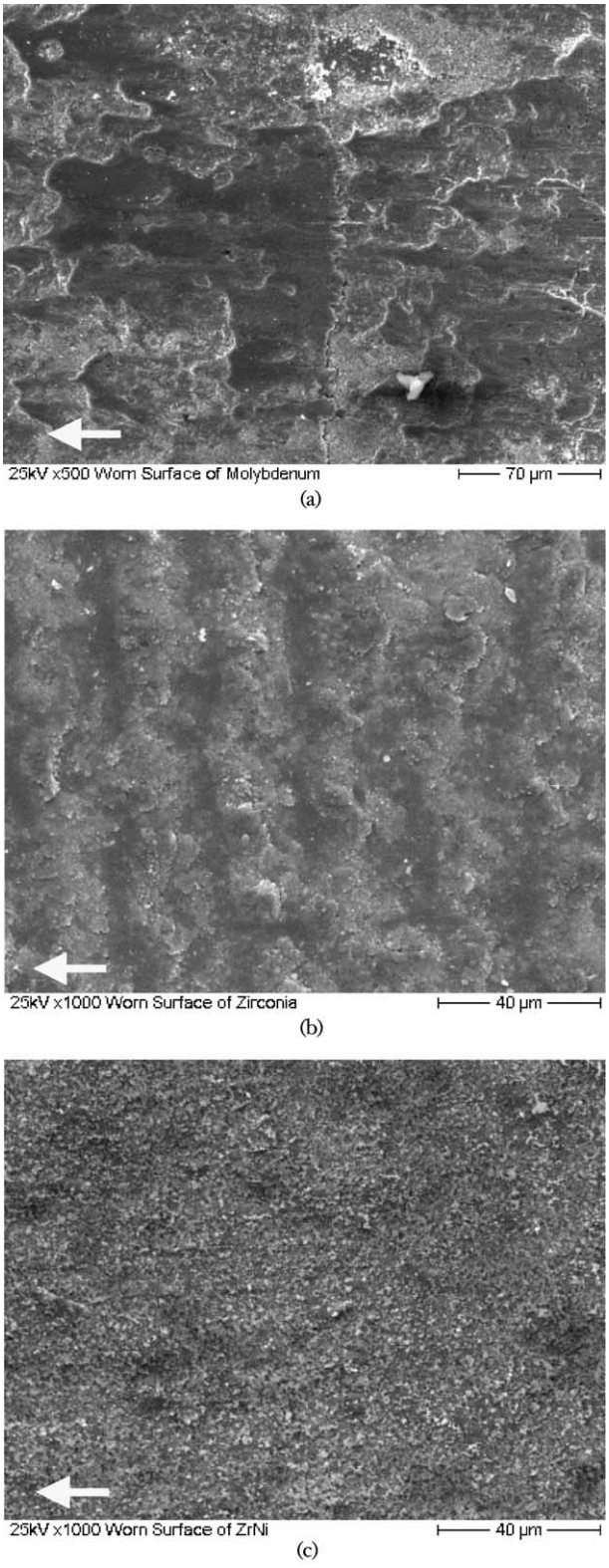

Fig. 6. The detailed worn aspects of (a) molybdenum, (b) zirconia and (c) zirconia/nickel composite (ZrO_2/Ni-2) after 72 km sliding.

4. Results and discussion

The densities and the universal and Vickers hardnesses of all the materials are summarised in Table 1. The relative densities of the sintered materials are also listed. The samples obtained have nearly reached their theoretical densities. The relative density of ZrO_2/Ni-2 was lower than the other sintered materials, and this may affect on the microhardness to result in the higher (quasi-)plastic deformation. As the Vickers hardness of mullite was almost twice as high than the universal hardness, this shows that the amount of the elastic deformation is almost the same as the (quasi-)plastic deformation. On the other hand, Mo and Ni deform only plastically, since both metals showed the same values for the universal hardness and the Vickers hardness.

The coefficients of friction of the systems, the specific wear rates of the pins, the cumulative wear rates of the steel discs and the total cumulative wear rates of the tribocouples are shown in Figs. 1–4. There was no remarkable difference in the coefficients of friction despite of the various tribocouples (Fig. 1). As for the sliding wear properties of the materials, mullite showed lower wear rate (2–4 times better) than the pure metal (Mo) or the composites (Mu/Mo-3, Mu/Mo-9). In addition, the particle sizes of the loaded metal significantly affected the wear rate of the composite. Zirconia showed also lower wear rate (16 times better) than the composite (ZrO_2/Ni-2) (Fig. 2). On the other hand, the wear rates of steel against mullite was 2–6 times higher than those against Mo, Mu/Mo-3 or Mu/Mo-9. Moreover, the wear rates of steel against Mu/Mo-3 and Mu/Mo-9 were lower than the one against Mo. Also, the wear resistance of steel against ZrO_2/Ni-2 probed to be 3.5 times better than the one against Zirconia (Fig. 3). Considering the total cumulative wear rate of the tribocouple (pin and disc), Mu/Mo-9 showed 2–3 times better wear performance than mullite, Mo and Mu/Mo-3. By contrast, ZrO_2/Ni-2 resulted in 1.8 times higher wear rate than zirconia (Fig. 4).

From the observations by SEM with WDX, which are shown in Fig. 5, the surface films found on all the worn sample pins indicated a clear transfer of iron from the steel counterparts. The sliding direction of the pin was indicated in the picture. It is evident that the amount of the transferred iron on the ceramic/metal composites was higher than that on the monolithic ceramics. Most probably these tribofilms consist of iron oxides,[13,15] which may play an important role on the wear mechanism, but further investigations on this matter are needed by using the energy dispersive X-ray quantitative analysis. Fig. 6 shows the SEM micrographs of Mo,

zirconia and ZrO_2/Ni-2 after sliding. On the worn surface of Mo, the ductile deformation of metal extrusions can be observed, whereas, on the worn surface of Zirconia, brittle fracture events, typical for monolithic ceramics, are found. The magnitude of the fracture on the worn surface of ZrO_2/Ni-2 is clearly smaller (smoother) than in case of the other materials, and this is attributed to the microstructure of the composite. For the metal–metal configuration as a tribocouple, adhesive wear is predominant, but for the ceramic–metal

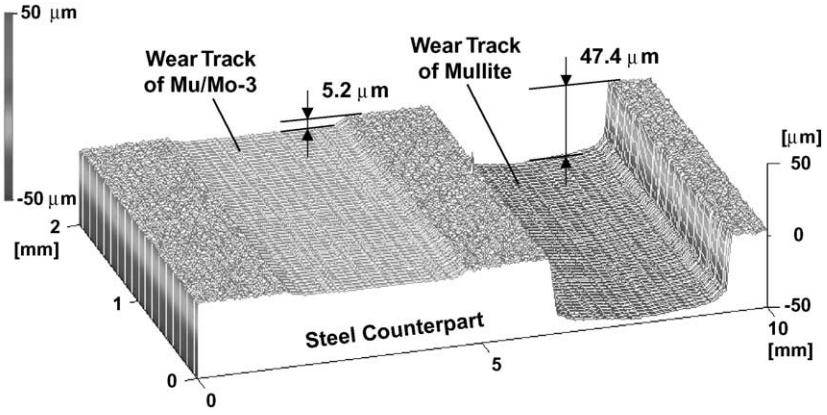

Fig. 7. Three-dimensional topographic map of the worn steel counterpart against mullite and mullite/molybdenum composite (Mu/Mo-3).

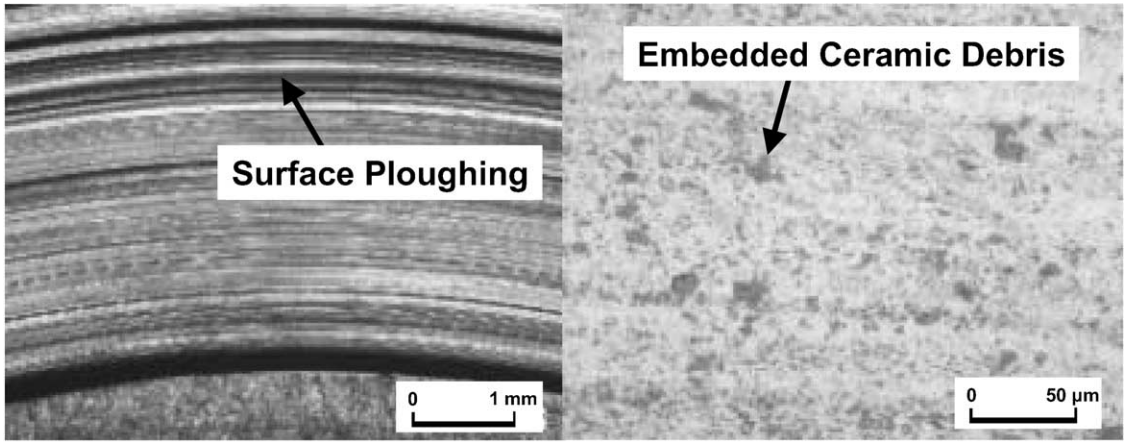

(a)

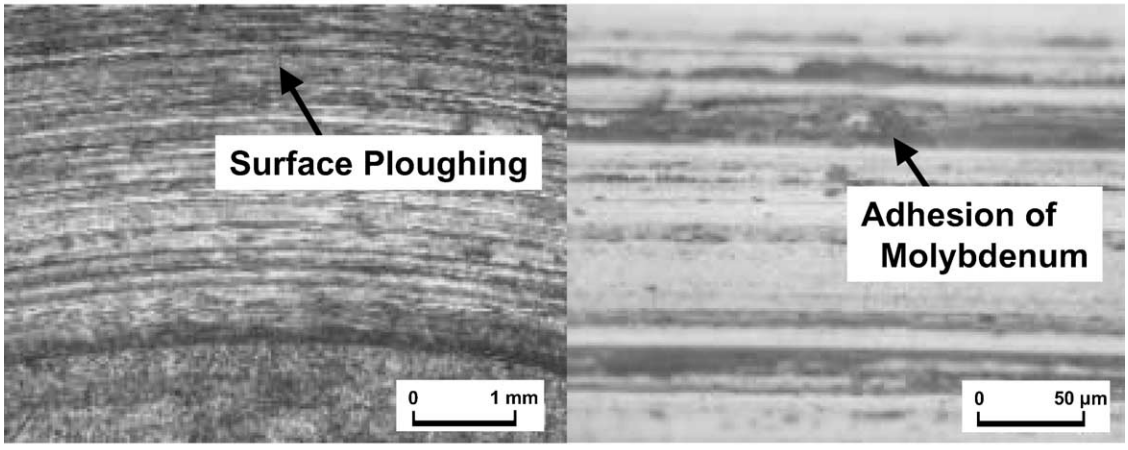

(b)

Fig. 8. Wear tracks of (a) mullite and (b) mullite/molybdenum composite (Mu/Mo-3) on steel counterpart.

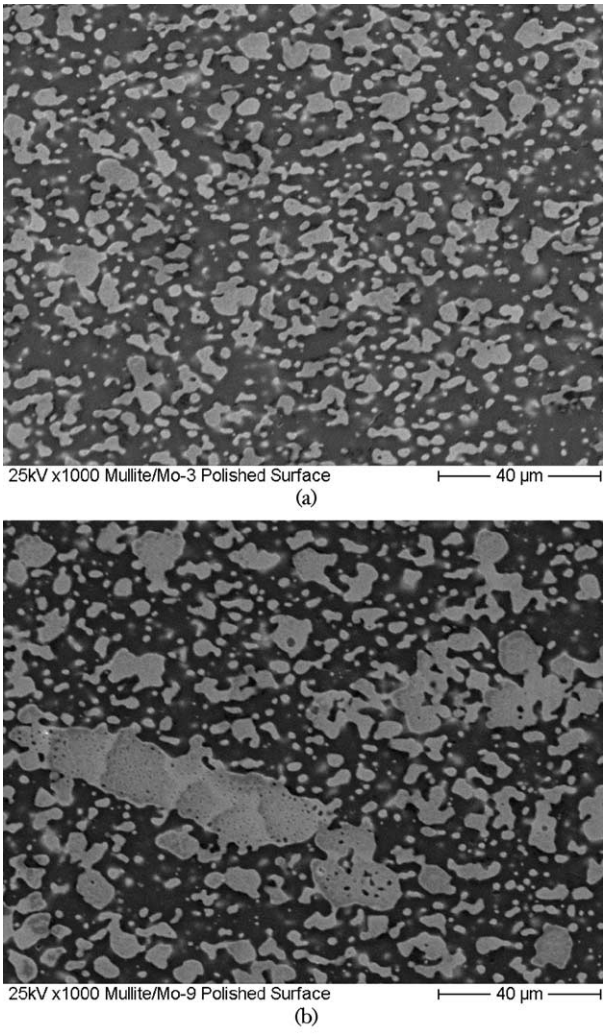

Fig. 9. Morphology of metallic phases in the polished mullite/molybdenum composites with different sizes of metal particles; (a) Mu/Mo-3 (32 vol.% Mo) and (b) Mu/Mo-9 (32 vol.% Mo). The dark area in the image is mullite, and the bright particles are Mo phase.

configuration, abrasive wear is also a major mechanism to be considered.

The three-dimensional topographic map of the wear tracks made by Mullite and Mu/Mo-3 on the steel counterpart using a laser surface profilometer is shown in Fig. 7. Both wear tracks were created under the same conditions, i.e. with the same applied load, speed and duration (distance). The depth of the wear track by mullite was nine times larger than that by Mu/Mo-3. It is obvious that the steel counterpart is severely worn out against monolithic ceramics, whereas the wear of the steel can be suppressed by incorporating a metal phase into the ceramic as a sliding body. The typical aspects of wear tracks on the steel counterpart by mullite and Mu/Mo-3 are shown in Fig. 8. Abrasive scars of surface ploughing were observed on every wear track. In addition, embedded ceramic wear debris was found on the wear tracks created by the monolithic ceramics. On the other hand, adhesion of metal from the pin material was found on the wear tracks created on the steel counterpart by the metal and ceramic/metal composite pins.

In order to discuss the wear mechanisms of the ceramic/metal composites, the microstructures of the composites must be considered. Fig. 9 shows the microstructures of the polished mullite/molybdenum composites with different sizes of metal particles. The metal phases are homogeneously distributed in the ceramic matrix, but the metal particles have complicated shapes, since they agglomerate during sintering with microscopically disordered neighbouring particles.[20] It must be noted that relatively huge polycrystalline agglomerates exist in Mu/Mo-9. In case of the relatively simple configuration of ceramic against metal, abrasive wear of the counterpart caused by the harder ceramic asperities or cracked-out ceramic particles (wear debris) is predominant, although adhesive wear of metal onto the ceramic can also occur (Fig. 10a). In the

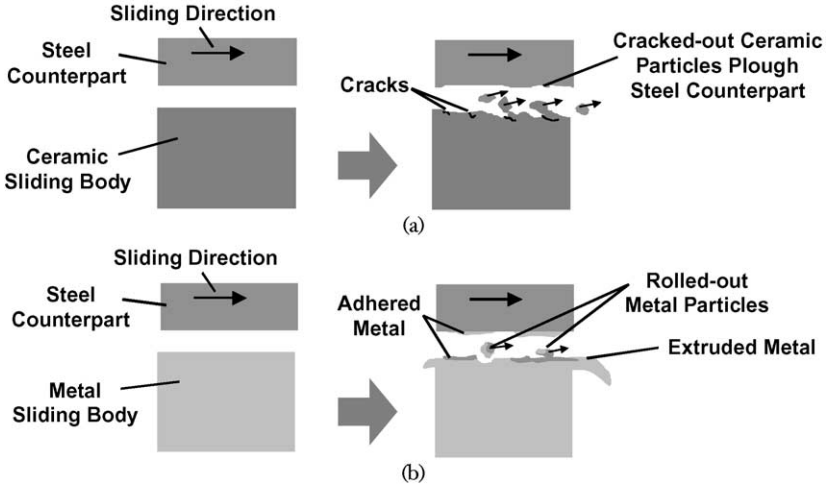

Fig. 10. Sliding wear mechanisms of (a) ceramic and (b) metal against steel.

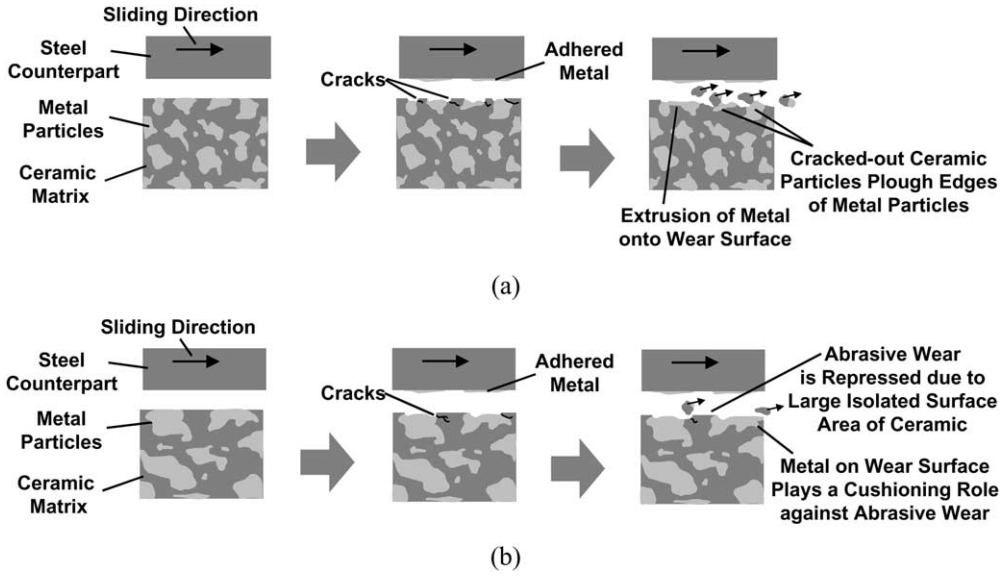

Fig. 11. Sliding wear mechanisms of mullite/molybdenum composites with (a) smaller and (b) larger sized metal particles.

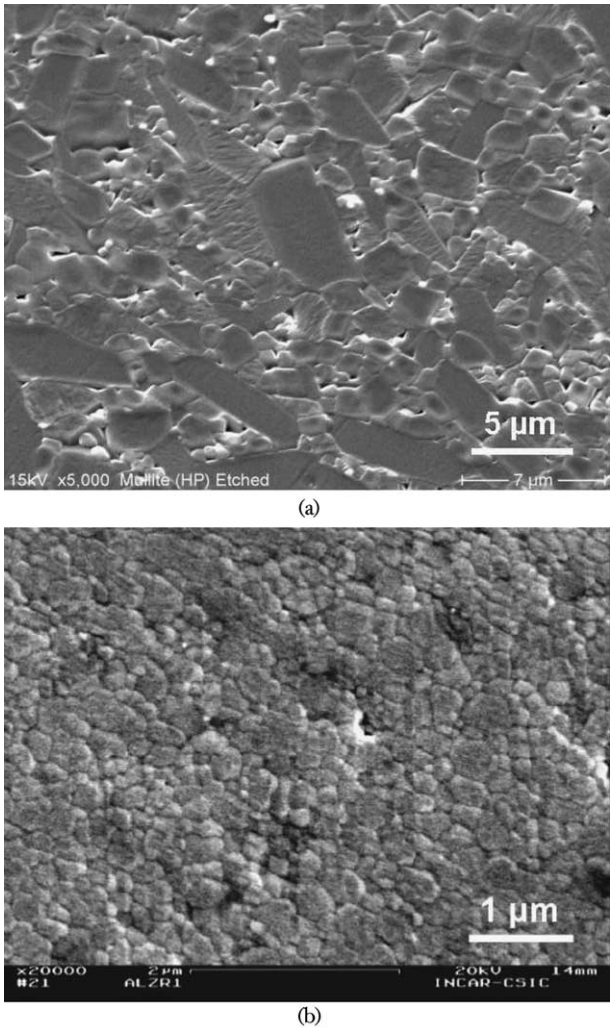

Fig. 12. Grain structures on thermally etched surfaces of monolithic (a) mullite and (b) zirconia.

case of metal against metal (here, molybdenum against steel), adhesion between the two metals takes place, and rolled-out metal particles (0.5–5 μm) are created under friction. A surface layer of metal is also dragged and extruded (Fig. 10b). The specific wear rate of the molybdenum was twice as high than the cumulative wear rate of the steel, because the hardness of the steel was ca. twice as high than that of molybdenum.

As it may be expected, the wear mechanism of the ceramic/metal composites is a combination of abrasive wear by hard ceramic asperities and particles and adhesive wear between the metallic components. Schematic drawings of the wear mechanisms of the ceramic/metal composites with different sizes of the metal phase in the composite are shown in Fig. 11. In the initial wear stage of a composite, metal adheres to the steel counterpart. At the same time, microcracks in the ceramic phase occur and propagate gradually on the scale of the surface roughness. The complex wear mode of an adhesion of metals and an abrasion of ceramic wear debris occurs, in which cracked-out ceramic particles plough through the metal phases. In addition, extruded tribofilms of metal on the worn surfaces are created. If the ceramic composites possess larger sized metal particles (in the case of Mu/Mo-9), abrasive wear is, however, suppressed, because the isolated areas of both the ceramic and the metal phases on the sliding surface are larger than the composites with smaller sized metal particles (Mu/Mo-3). The surface asperities of the ceramic are progressively damaged by the same amount of energy from abrasive particles or asperities as the composite with smaller sized metal particles. This means, the size of the grown microcracks in the ceramic phase is the same in both composites. Here, it is supposed that the grain size and shape of the ceramic phase and the

number of asperities are similar in both composites. Moreover the area of the adhered and extruded metal on the sliding surface, which can deform plastically and absorb impact energy, i.e. it plays a cushioning role against hard particle abrasion, is larger than the composite with smaller sized metal particles. At the same time, the presence of ceramic prevents the occurrence of adhesive wear of the various metals. The importance of the oxides, which act as hard abrasive particles against metal, was also focused and reported in

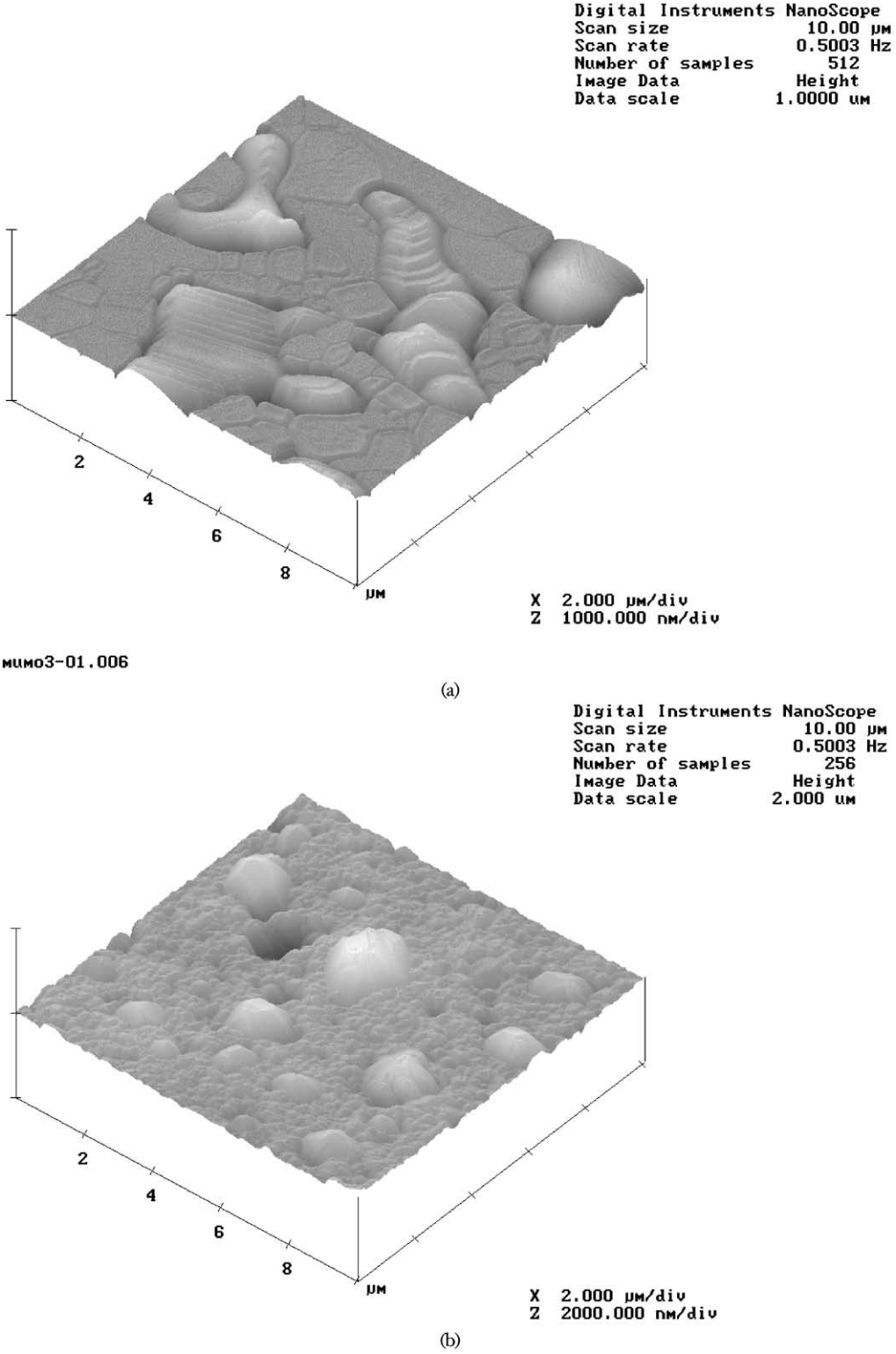

Fig. 13. Grain structures on thermally etched surfaces of (a) mullite/molybdenum (Mu/Mo-3) and (b) zirconia/nickel (ZrO_2/Ni-2) composites.

Ref. 15. Hence, it is worth mentioning that the size and the amount of the metal phase are the key to control the wear of a ceramic/metal composite in a desirable condition.

For a comparison between the mullite/molybdenum composite and the zirconia/nickel composite, a SEM photograph of the thermally etched surface of the monolithic mullite and the detailed grain structures of the thermally etched composites by AFM are shown in Figs. 12 and 13, respectively. Figs. 12a and 13a prove that the mullite/molybdenum composite has quite complicated shapes of the metal phase, which, in turn, build-up an interlocking structure with the irregular shapes of the ceramic grains. Furthermore, the mullite/molybdenum interfaces are strongly bonded.[16] These facts promote the plastic deformation of the ductile phase and prevent the ceramic–metal debonding. With this structure, microcracks pass through the ceramic grains and metal particles are mechanically interlocked in the ceramic phase, so that they can work as a crack shielding material. This brought about the better wear resistance for the ceramic/metal composites. On the other hand, as shown in Figs. 12b and 13b, the zirconia/nickel composite has equiaxial (quasi-spherical) and regular shapes of the metal and the ceramic grains. Additionally, the zirconia/nickel interfaces are weak,[18] and therefore the microcracks will be generated between the ceramic grain boundaries and at the ceramic/metal interface. Hence, the ceramic grains as well as the metal particles are easily dug out from the system under friction. It is inferred that the smooth worn surface in Fig. 6c is attributed to this mechanism.

In conclusion, it can be therefore stated here, that it is important to pay attention on the microstructural factors, such as the volume fraction, the sizes and the shapes of the metal phase and the ceramic grains in a ceramic/metal composite as a tribomaterial. The influence of the amount and the size of metal phase in a ceramic/metal composite and the oxidation of the tribofilms will be studied in more detail in a future work.

5. Conclusions

The sliding wear behaviour of monolithic ceramics (mullite, zirconia), pure metal (molybdenum) and ceramic/metal composites (mullite/molybdenum, zirconia/nickel) with different sizes and morphology of the metal particles was studied. If a ceramic contains a metallic phase (i.e. if one deals with a ceramic/metal composite), the wear of the steel counterpart is drastically reduced at the cost of a higher wear of the composite pin. In the case of the Mu/Mo-9 composite, the total cumulative wear rate (the wear rate of both the sliding body and its steel counterpart) is twice as good than the other systems, i.e. the monolithic mullite, the pure molybdenum and the Mu/Mo-3 composite against steel.

Both the particle size and shape of the metallic phase and ceramic matrix, as well as the characteristic of the bonding between different components in a composite are very important factors in order to control the wear of the composite. From the results obtained in this study, it can be concluded that tribo-materials and systems based on ceramic/metal composites can be microstructurally designed and optimised in order to control effectively the wear of both the sliding body and its counterpart.

Acknowledgements

The authors gratefully acknowledge the financial support of the Stiftung Industrieforschung, Köln, Germany (T10/2000). Further thanks are due to the German Academic Exchange Organization (DAAD) for support of the German-Spanish cooperation (Project No. 4531). Further thanks are due to the Spanish Ministry of Science and Technology for financial support under project MAT2000-1354 and for the Cooperation Project HA2000-0069.

References

1. *The American Ceramic Society Fact Sheets* http://www.ceramics.org/news/factsheets.asp.
2. Heinrich, J. G., Aldinger, F., ed., *Ceramic Materials and Components for Engines*. Wiley-VCH, Weinheim, 2001.
3. Krstic, V. D., On the fracture of brittle-matrix/ductile-particle composites. *Philosophical Magazine A*, 1983, **48**, 695–708.
4. Sigl, L. S., Mataga, P. A., Dalgleish, B. J., McMeeking, R. M. and Evans, A. G., On the toughness of brittle materials reinforced with a ductile phase. *Acta metall.*, 1988, **36**, 945–953.
5. Bannister, M. and Ashby, M. F., The deformation and fracture of constrained metal sheets. *Acta Metall. Mater.*, 1991, **39**, 2575–2582.
6. Bowden, E. P. and Tabor, D., *The Friction and Lubrication of Solids, 2nd. edn*. Clarendon Press, Oxford, 1954.
7. Sarkar, A. D., *Wear of Metals*. Pergamon Press, Oxford, 1976.
8. Kragelski, I. V., Dobyèin, M. N. and Kombalov, V. S., *Friction and Wear Calculation Methods*. Pergamon Press, Oxford, 1982.
9. Zum Gahr, K. H., *Microstructure and Wear of Materials*. Elsevier, Amsterdam, 1987.
10. Sekiguchi, I., Norose, S. and Nitanai, A., *Tribomaterial Katsuyou-Note*. Kogyo Chosakai, Tokyo, 1994 (in Japanese).
11. Hawthorne, H. M., and Troczynski, T. (Eds.) In *Proceedings of the International Symposium on Advanced Ceramics for Structural and Tribological Applications, Vancouver, Aug. 20–24, 1995*.
12. Bhushan, B., ed., *Modern Tribology Handbook, Vol. 1 Principles of Tribology*. CRC Press, Boca Raton, 2001.
13. Ravikiran, A., Jayaram, V. and Biswas, S. K., Sliding wear of Al_2O_3–SiC–(Al,Si) composites against a steel counterface. *J. Am. Ceram. Soc.*, 1997, **80**, 219–224.
14. Alman, D. E. and Hawk, J. A., Abrasive wear behavior of a brittle matrix ($MoSi_2$) composite reinforced with a ductile phase (Nb). *Wear*, 2001, **251**, 890–900.
15. Varenberg, M., Halperin, G. and Etsion, I., Different aspects of the role of wear debris in fretting wear. *Wear*, 2002, **252**, 902–910.
16. Bartolomé, J. F., Díaz, M., Requena, J., Moya, J. S. and Tomsia,

A. P., Mullite/molybdenum ceramic-metal composites. *Acta Mater.ialia*, 1999, **47**, 3891–3899.
17. Bartolomé, J. F., Díaz, M. and Moya, J. S., Influence of the metal particle size on the crack growth resistance in mullite/molybdenum composites. *J. Am. Ceram. Soc.*, 2002, **85**, 2778–2784.
18. López-Esteban, S., Bartolomé, J. F., Moya, J. S. and Tanimoto, T., Mechanical performance of 3Y-TZP/Ni composites: tensile, bending and uniaxial fatigue tests. *J. Mater. Res.*, 2002, **17**, 1592–1600.
19. *ASTM G99-95*. Standard Test Method for Wear Testing with a Pin-on-Disk Apparatus.
20. Pecharromán, C., López-Esteban, S., Bartolomé, J. F. and Moya, J. S., Evidence of nearest-neighbor ordering in wet-processed zirconia–nickel composites. *J. Am. Ceram. Soc.*, 2001, **84**, 2439–2441.